Macromolecules
ARTICLE

Macromolecules **2009**, *42*, 8943–8949 **8943**
DOI: 10.1021/ma9017108

Cerium(III) as a Stabilizer of Perfluorinated Membranes Used in Fuel Cells: In Situ Detection of Early Events in the ESR Resonator

Marek Danilczuk,[‡] Shulamith Schlick,*[,‡] and Frank D. Coms[§]

[‡]*Department of Chemistry and Biochemistry, University of Detroit Mercy, 4001 West McNichols Road, Detroit, Michigan 48221, and* [§]*General Motors Electrochemical Energy Research Lab, 10 Carriage Street, Honeoye Falls, New York 14472*

Received July 31, 2009; Revised Manuscript Received September 24, 2009

ABSTRACT: We present experiments in an in situ fuel cell (FC) inserted in the resonator of the ESR spectrometer that allowed separate monitoring of radical formation at anode and cathode sides. The in situ FC was operated at 300 K under closed and open circuit voltage conditions, CCV and OCV, respectively, with a membrane-electrode assembly (MEA) based on Nafion 117 10% neutralized by Ce(III) and Pt as catalyst, notation MEA/Ce. The presence of the unstable intermediates was determined by addition of 5,5-dimethylpyrroline-*N*-oxide (DMPO) as a spin trap, simulation of the spectra from the DMPO adducts, and analysis of the corresponding magnetic parameters and relative intensities. The main objective of these experiments was to identify *early events* in the mitigation mechanism of Ce(III) on Nafion degradation. The present results were therefore compared to an in situ FC based on Nafion 117 in the acid form, notation MEA/H (Danilczuk et al. *J. Phys. Chem. B* **2009**, *113*, 8031−8042) that served as baseline. The differences between the two types of experiments are significant. (a) Spin trapping indicated the presence of different radicals: $HO^{\bullet}$ for MEA/H and $HOO^{\bullet}$ for MEA/Ce. (b) DMPO/CCR, the adduct of a carbon-centered radical (CCR) generated by membrane fragmentation, is absent for the MEA/Ce FC, but was detected in the MEA/H FC under similar operating conditions. (c) The intensity of all adducts is much lower in the MEA/Ce FC. The *absence* of DMPO/OH for MEA/Ce was explained by scavenging of the aggressive $HO^{\bullet}$ radicals by Ce(III); this process also generates Ce(IV). The *presence* of DMPO/OOH for MEA/Ce was rationalized by Ce(IV) oxidation of H_2O_2 leading to the formation of $HOO^{\bullet}$. The *absence* of DMPO/CCR is a result of $HO^{\bullet}$ scavenging and the formation of the less aggressive oxidant, $HOO^{\bullet}$, in MEA/Ce. The low intensity of all adducts is also a result of $HO^{\bullet}$ scavenging by Ce(III). Ce(III) is an effective stabilizer because of the Ce(III)/Ce(IV) couple redox chemistry, which allows significant stabilization with a low stabilizer concentration.

Introduction

The durability of proton exchange membranes (PEMs) used in fuel cells (FCs) is a major problem that must be solved before the broad introduction of these energy converters in automotive and other applications. Until very recently the membranes did not fulfill the automotive demands, which require that the membrane demonstrate a stability greater than ≈ 5500 h under normal operating conditions.[1] The effect of neutralizing cations on the rate of membrane degradation has been investigated in great detail. Recent FTIR and ^{19}F NMR results have suggested that the durability of Nafion (Chart 1) neutralized by alkali and alkaline earth metal ions is similar to that of Nafion in the acid form.[2] The effect of transition metal cations such as Fe(II), Cu(II), Cr(III), and Co(II) has been compared: The membrane degradation rate was highest in the case of Fe(II).[2] This result was rationalized by a Fenton reaction between the cation and hydrogen peroxide,[3] H_2O_2, which is known to be formed at the cathode side of the FC by the two-electron oxygen reduction reaction (#1 below). The Fenton reaction leads to the formation of hydroxyl ($HO^{\bullet}$) and hydroperoxyl ($HOO^{\bullet}$) radicals (reactions 2 and 3 below), which are involved in reactions leading to membrane degradation.[4]

$$O_2 + 2H^+ + 2e^- \rightarrow H_2O_2 \text{ (at the cathode)} \quad (1)$$

$$H_2O_2 + Fe(II) \rightarrow HO^{\bullet} + HO^- + Fe(III) \quad (2)$$

$$H_2O_2 + HO^{\bullet} \rightarrow HOO^{\bullet} + H_2O \quad (3)$$

The structure of radicals generated by fragmentation of Nafion membranes neutralized by Fe(II) has been determined by our group via electron spin resonance (ESR): Strong signals from a chain-end radical $RCF_2CF_2^{\bullet}$ were detected at 77 K in UV-irradiated Nafion/Fe(III).[5] Fitting of the ESR spectrum together with density functional theory (DFT) calculations have indicated that the radical formed is $ROCF_2CF_2^{\bullet}$, as expected from a radical derived from the side chain of Nafion, not $RCF_2CF_2CF_2^{\bullet}$, if its origin is the main chain.[6] Additional support for this assignment was obtained from exposure of a model compound that mimics the Nafion side chain, perfluoro(2-ethoxyethane)sulfonic acid ($CF_3CF_2OCF_2CF_2SO_3H$, PFEESA), to $HO^{\bullet}$ radicals generated by UV-irradiation of H_2O_2.[7] In conclusion, our ex situ results have indicated that the Nafion side chain is vulnerable to attack by oxygen radicals. Strong support of this idea was reported recently in an in situ study of perfluorinated membranes by solid state ^{13}C and ^{19}F NMR spectroscopy; moreover, this study has suggested that "*the pendant side chains of the ionomers are more affected than the main chain*".[8]

The effect of transition metal cations is, however, not limited only to an *increased* rate of membrane degradation: Recent reports have disclosed the use of Ce(III) and Mn(II) ions as well as metal cerium oxides as powerful mitigants of chemical membrane degradations.[9,10] Moreover, the addition of small amounts

*Corresponding author. Telephone: 1-313-993-1012. Fax: 1-313-993-1144, E-mail: schlicks@udmercy.edu.

Published on Web 10/01/2009

Chart 1. Nafion 117, EW 1100

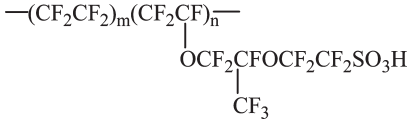

Scheme 1. Spin Trapping by 5,5-Dimethyl-1-pyrroline-*N*-oxide (DMPO)

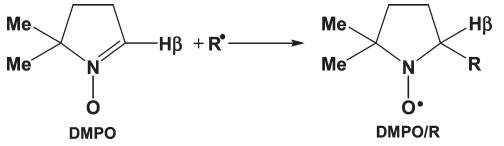

of Ce(III) to the membrane, typically $<1\%$ of membrane neutralization or ≤ 3 wt % of CeO_2 particles, did not affect the performance of the FC. Recent published data have provided support for the relative rate hypothesis: the reaction of Ce(III) with the aggressive $HO^{\bullet}$ radicals is faster than the reaction between $HO^{\bullet}$ radicals and the FC membrane, resulting in a protective effect.[11]

We present a study of the effect of Ce(III) on membrane degradation in an in situ fuel cell inserted in the variable temperature insert of the ESR resonator. The membrane-electrode assembly (MEA) was based on Nafion 10% neutralized by Ce(III), notation MEA/Ce. The major goal of this study was to detect early events in the stabilization process: unstable radical fragments generated during FC operation. The results of closed and open circuit voltage conditions, CCV and OCV respectively, were compared to recent results in the in situ FC based on Nafion in the acid form, notation MEA/H. For both MEA types, the presence of radical fragments was detected by spin trapping with 5,5-dimethylpyrroline-*N*-oxide (DMPO) as the spin trap.[12] The method is based on scavenging of short-lived radicals by spin traps and formation of more stable adducts, typically nitroxide radicals,[13,14] as shown in Scheme 1 for DMPO as the spin trap. In most cases the ESR spectra of DMPO spin adducts exhibit hyperfine splittings (hfs) from ^{14}N and H_{β} nuclei, a_N and a_H, respectively.[7,15,16] From these hfs it is often possible to determine the structure of the trapped radicals.

As described below, the major results of the MEA/Ce FC were as follows: the *presence* of $HOO^{\bullet}$ as the DMPO/OOH adduct at the cathode (CCV conditions); the *absence* of the carbon-centered radical adduct, DMPO/CCR (CCV conditions); the *lower intensity of all DMPO adducts*. These results are in contrast to results for the MEA/H FC. Analysis and comparison of the in situ results led to a better mechanistic understanding of Ce(III) mitigation and to the formulation of general requirements for effective membrane stabilization.

Experimental Section

Materials. The high purity DMPO spin trap was purchased from Alexis Biochemicals and used without further purification. The gases (H_2 99.99%, D_2 99.8%, O_2 99.6%), Pt mesh with $d = 0.1$ mm, and Ag wire with $d = 0.127$ mm were from Sigma-Aldrich. Membrane-electrode assemblies (MEA/Ce) based on Nafion (thickness 0.178 mm) and Pt as catalyst (coverage 0.2 mg/cm^2) were a gift from Cortney Mittelsteadt of Giner Electrochemical Systems, LLC, where they were prepared using the decal-transfer process, as described previously.[12] Ce(III) ions were introduced by ion exchange with the soluble cerium nitrate prior to MEA preparation, to a 10% degree of neutralization.

In Situ Fuel Cell. The FC consists of two half-cylinders made of polystyrene cross-linked with 1,4 divinylbenzene (Rexolite), with indentation where the membrane, the Pt mesh and the electrodes were placed.[12] The fuel cell was inserted in the variable temperature insert of the ESR spectrometer; the results presented here were obtained at 300 K, but temperature variation is possible and is planned for future experiments. The electrodes were connected to an HP E2377A multimeter by silver wires. The gas flows to the fuel cell, 2 mL/min for oxygen, and 4 mL/min for hydrogen and deuterium, were controlled with Matheson 610A flow meters. A schematic drawing of the in situ FC is shown in Supporting Information. Full details on the design and dimensions of the in situ FC are available from the authors upon request.

Spin Trapping of Radical Intermediates. DMPO was chosen as the spin trap because of its well-documented trapping ability for oxygen radicals and for carbon-centered radicals (CCRs).[7,13−16] Typically 1 μL of the aqueous solution of the spin trap, concentration 4 M, was deposited at the cathode or anode side; the solvent was H_2O for H_2 at the anode, and D_2O for D_2 at the anode. In some experiments the spin trap was added just before starting the FC operation. In other experiments, the FC was operated for 120−360 min, followed by addition of the DMPO solution and restarting of the gas flows; these results are expected to reflect the effect of MEA/Ce "break in" and membrane hydration on the type of radicals and adducts formed.

ESR Measurements. ESR spectra were recorded at 300 K using Bruker X-band EMX spectrometers operating at 9.7 GHz and 100 kHz magnetic field modulation, and equipped with the Acquisit 32 Bit WINEPR data system version 3.01 for acquisition and manipulation, and the ER 4111 VT variable temperature units. The microwave frequency was measured with the Hewlett-Packard 5350B microwave frequency counter. The hfs of the spin adducts were determined by fitting the spectra using the WinSim (NIEHS/NIH) simulation package;[17] the fitting also determines the relative intensity of each component for spectra that consist of a superposition of contributions from different adducts. The acquisition parameters for all ESR spectra were: sweep width 150 G, microwave power 2 mW, time constant 20.48 ms, conversion time 41.94 ms, modulation amplitude 2 G, receiver gain 1×10^5, 2048 points, and 50 scans. Additional experimental details are given in ref 12.

Results

The in situ experiments were performed at 300 K with the fuel cell operated at CCV and OCV conditions, with oxygen at the cathode and hydrogen or deuterium gas at the anode. No signals were detected before connecting the gases and addition of the spin trap solution on the membrane, or in the presence of the spin trap and the absence of the gases. As in ref 12, numerous experiments have showed that applying the spin trap solution at one electrode leads to the formation of adducts *at that electrode only*. Therefore, the results, presented in Figures 1−4, will be described for DMPO applied on the cathode or anode side, with the indicated gases fed at electrodes; experimental ESR spectra are in black and simulated spectra are in blue. Ce(III) is a $4f^1$ ion with a ground state of $^2F_{5/2}$; because of fast spin−lattice relaxation time, the ESR spectrum of $CeCl_3$ in a sample with La(III) as the diamagnetic diluent was detected only at low temperatures, typically 4.2 K.[18] Therefore, no ESR spectrum is expected from Ce(III) at 300 K.

Cathode H_2/O_2. Figure 1A presents the evolution of ESR spectra of DMPO adducts when the spin trap was introduced to the cathode side of MEA/Ce FC just before CCV operation ("0 min") and after operating times of 120, 240, and 360 min. The DMPO/OOH adduct (a_N = 13.6 G, a_H = 11.3 G) is dominant for "0 min" and 120 min conditions. However, the dominant signal detected after 240 and 360 min is the DMPO/H adduct with hfs from ^{14}N and from two equivalent ^1H nuclei (a_N = 14.8 G, a_H = 19.8 G, (2H)). Experimental and simulated ESR spectra after 360 min of

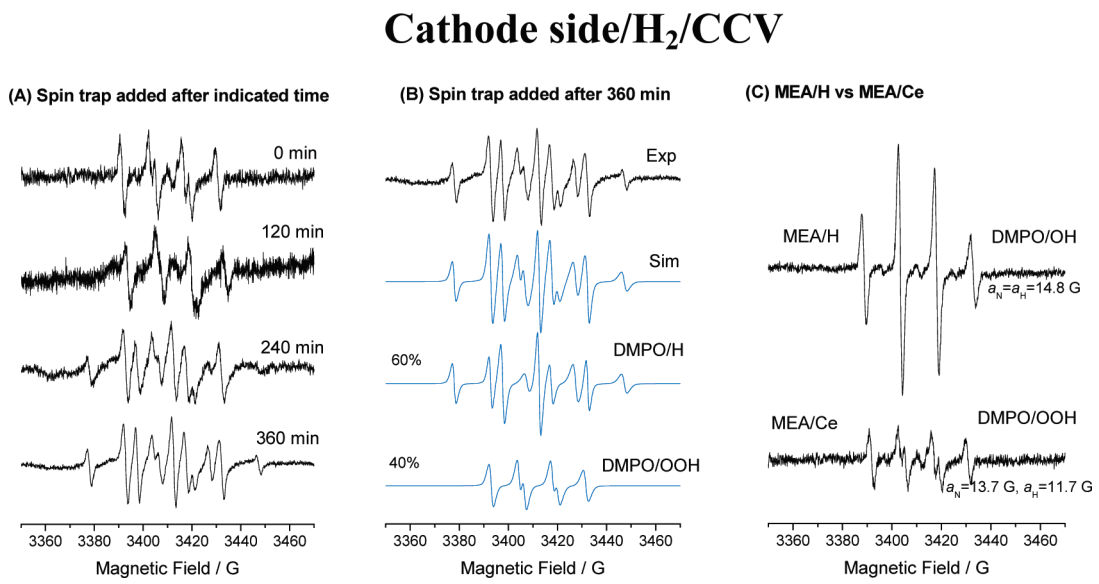

Figure 1. (A) Time evolution of ESR spectra of DMPO adducts at the cathode side, CCV operation in the in situ FC, with H_2 at the anode. For the top spectrum "0 min" indicates that the spin trap was added just before FC operation. For the other spectra the spin trap was added after the indicated operation time. (B) Experimental and simulated ESR spectra of adducts when the spin trap was added after 360 min of operation. The relative intensity of each adduct is shown on the left. (C) Comparison of DMPO adducts detected with the MEA/H (top) and with MEA/Ce (bottom). Note the different hyperfine splittings for the two adducts and the lower signal intensity in the MEA/Ce FC. See text.

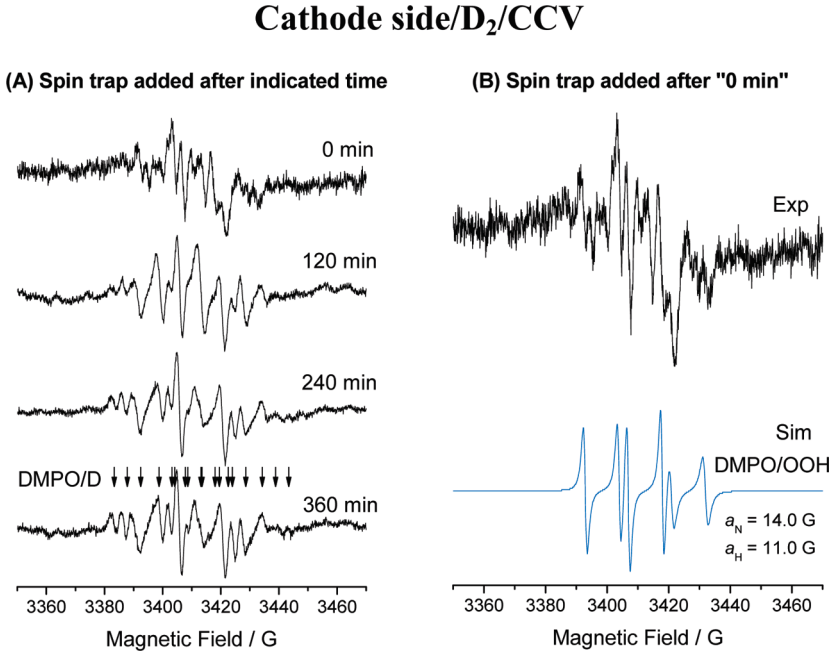

Figure 2. (A) Time evolution of ESR spectra of DMPO adducts at the cathode side, CCV operation in the in situ FC, with D_2 at the anode. In the top spectrum "0 min" indicates that the spin trap was added just before FC operation. For the other spectra the spin trap was added after the indicated operation time. In the bottom spectrum arrows indicate the signals expected from the DMPO/D adduct. (B) Experimental and simulated ESR spectra of the DMPO/OOH adduct present for "0 min" operation. See text.

CCV operation are shown in Figure 1B. The experimental spectrum was simulated as a sum of two components: the DMPO/H adduct (60% relative intensity) and the DMPO/OOH adduct (40% relative intensity). The hfs of all adducts are in line with the literature data.[16,19−21]

Figure 1C compares ESR spectra of adducts detected for the same experimental conditions ("0 min", spin trap added just before FC operation) and acquisition parameters in the in situ MEA/H and MEA/Ce FCs. The differences are significant and are clearly a result of (partial) membrane neutralization by Ce(III): (a) The dominant adducts are different: DMPO/OH for the MEA/H FC (a_N = a_H = 14.8 G)[12] and DMPO/OOH for MEA/Ce FC (a_N = 13.7 G and a_H = 11.7 G). (b) The DMPO/CCR adduct, the adduct of a carbon-centered radical derived from the membrane, is absent for MEA/Ce FC, while in the absence of Ce(III) it was detected after operating times ≥240 min. In the Supporting Information we present experimental and simulated ESR spectra of adducts measured after CCV operation time of 240 min for the MEA/H FC, in which the relative intensity of the DMPO/CCR adduct is 29%.[12] (c) The intensity of all adducts is much lower in the MEA/Ce FC.

Cathode (D_2/O_2). Figure 2A presents the ESR spectra of DMPO adducts when the spin trap was introduced to the

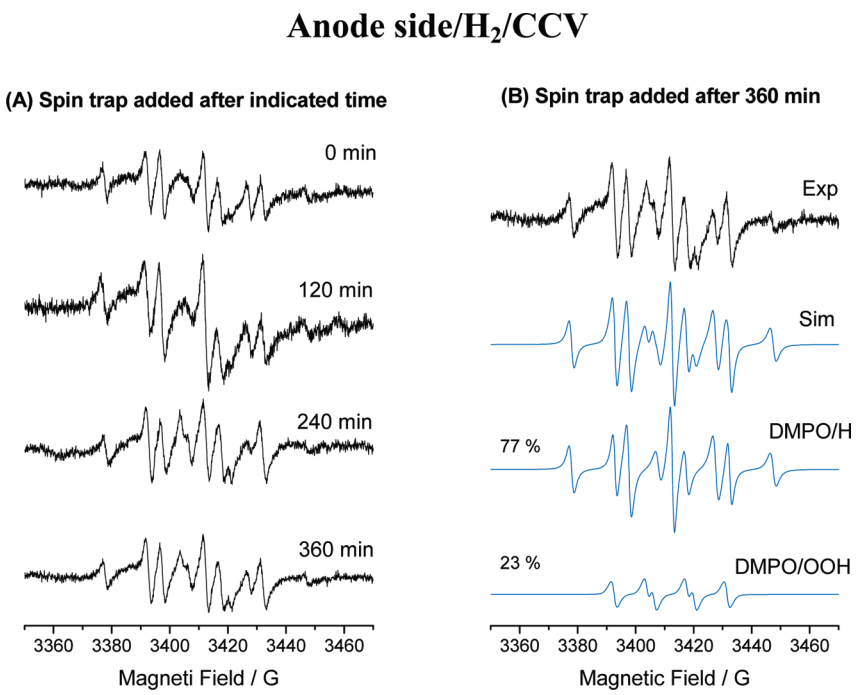

Figure 3. (A) Time evolution of ESR spectra of DMPO adducts at the anode side, CCV operation, with H_2 at the anode. In the top spectrum "0 min" indicates that the spin trap was added just before FC operation. For the other spectra the spin trap was added after the indicated operation time. (B) Experimental and simulated ESR spectra of adducts when the spin trap was added after 360 min of operation. The relative intensity of the two adducts is shown on the left. See text.

cathode side just before CCV FC operation ("0 min") and after operation times of 120, 240, and 360 min. The signal from the DMPO/D adduct appears for operating times ≥120 min; arrows in the bottom spectrum point to the expected signals for the DMPO/D adduct: a_N = 16.0 G, a_H = 20.8 G (1H), and a_D = 3.3 G (1D). Experimental and simulated ESR spectra after "0 min" of CCV operation are shown in Figure 2B. The spectral intensity is low, but the major signal can be assigned to the DMPO/OOH adduct (a_N = 14.0 G, a_H = 11.0 G). As for the CCV results with H_2 at the anode, Figure 1, we note the absence of the DMPO/CCR adduct.

Anode H_2/O_2. The ESR spectra recorded for CCV conditions with DMPO at the anode side are shown in Figures 3. Figure 3A presents the evolution of ESR spectra of DMPO adducts when the spin trap was introduced just before FC operation ("0 min") and after operation times of 120, 240, and 360 min. The dominant signal is the DMPO/H adduct. For FC operation ≥240 min, the additional weak signal of DMPO/OOH appeared. Figure 3B presents the experimental and simulated ESR spectra after 360 min of CCV operation. The simulation is a sum of two components: the dominant signal of the DMPO/H adduct (a_N = 15.0 G, a_H = 20.0 G (2H), relative intensity 77%) and the DMPO/OOH adduct (a_N = 13.6 G, a_H = 11.3 G, relative intensity 23%). The results are similar to those obtained for the MEA/H-based FC in terms of the dominance of the DMPO/H adduct; the difference is the detection of the weak DMPO/OOH signal in the MEA/Ce-based FC.

Anode D_2/O_2. Figure 4A presents ESR spectra of adducts detected when the spin trap was added just before starting FC operation ("0 min") and after CCV operation times of 120, 240, and 360 min with D_2 at the anode. Figure 4B presents the experimental and simulated ESR spectra after 360 min of CCV FC operation. The experimental spectrum was simulated as a sum of two components: the dominant signal from the DMPO/D adduct (a_N = 15.1 G, a_H = 20.0 G, a_D = 3.3 G, relative intensity 80%), and the weaker contribution from the DMPO/H adduct (a_N = 15.0 G, a_H = 20.1 G (2H), relative intensity 20%). The results at the anode are similar to those obtained for MEA/H-based FC, but the relative intensity of the DMPO/D adduct is higher, 80% vs 32%.

For OCV conditions and DMPO at the cathode or anode, only very weak signals were detected and analysis of adducts was not possible.

Discussion

In this section, we will discuss the major experimental results shown in Figures 1−4: the *presence* of the DMPO/OOH adduct and the *absence* of the DMPO/CCR adduct at the cathode for CCV operation and the very low ESR intensity of *all detected adducts*. These results for the MEA/Ce FC will be compared to those deduced for the MEA/H FC as a baseline.[12]

Discussion of the chemical mitigation mechanism by Ce(III) must be considered in the context of what is known on the chemical degradation of Nafion and other perfluorinated ionomeric membranes with sulfonic acid end groups (PFSA), and of relevant model compounds.[5−8,22−27] It is widely accepted that chemical degradation of these ionomers can be initiated via a main chain unzipping process which begins with hydrogen atom abstraction from either an end group carboxylic acid present as an impurity or from a hydrofluorocarbon group by oxygen radicals; the unzipping mechanism is shown in Supporting Information. In addition, important evidence for membrane fragmentation by $HO^•$ attack of the side chains has been published recently;[5−8,25,26] these ideas are in agreement with our most recent spin trapping ESR studies of model compounds that mimic the Nafion side chain.[7,28] For both main chain and side chain attack sites, the hydroxyl radical appears to be the *only* oxidant capable of initiating the fragmentation of the PFSA membranes and of model compounds.[27] The higher reactivity of $HO^•$ relative to $HOO^•$ is reflected in their respective reduction potentials (2.59 vs 1.48 V) and the O−H bond strengths of their corresponding reduced forms H_2O and H_2O_2 (497 vs 369 kJ/mol). Attack by $HO^•$ explained the results of in situ FC experiments

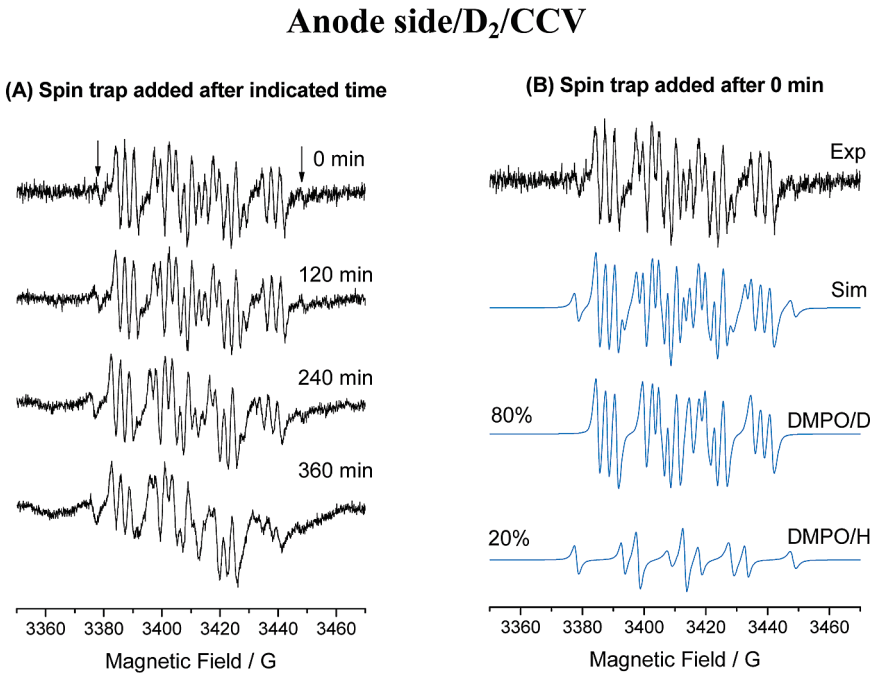

Figure 4. (A) Time evolution of ESR spectra of DMPO adducts at the anode side, CCV operation, with D_2 at the anode. In the top spectrum "0 min" indicates that the spin trap was added just before FC operation, and downward arrows point to lines at the lowest and highest field from the DMPO/H adduct. (B) Experimental and simulated ESR spectra of adducts when the spin trap was added after "0" min of operation: DMPO/D (a_N = 15.1 G, a_H = 20.0 G, a_D = 3.1 G, 80%), and DMPO/H (a_N = 15.0 G, a_H = 20.0 G, 20%). See text.

with the MEA/H.[12] In this section we will rationalize the results for the MEA/Ce FC.

The Absence of DMPO/OH and DMPO/CCR Adducts at the Cathode for CCV Operation. As seen in Figures 1 and 2, the DMPO/OOH adduct was detected at the cathode side for CCV conditions with H_2 or D_2 at the anode. The situation was different in the MEA/H FC, where DMPO/OH was detected. From simulations of the spectra shown in Figure 1C we have deduced that the intensity ratio of DMPO/OH in the MEA/H FC to that of DMPO/OOH in the MEA/Ce FC is 89/11; the intensity of *all* adducts in the MEA/Ce FC is very low.

Another major result in Figures 1 and 2 is the *absence* of DMPO/CCR, the adduct of a carbon-centered radical derived from the membrane, which was detected in the MEA/H FC.[12] Taken together, these results suggest that the concentration of the aggressive $HO^\bullet$ radicals is much lower in the MEA/Ce FC.

If the formation of $HO^\bullet$ radicals cannot be prevented in an operating fuel cell, the radicals must be deactivated or quenched faster than they induce damage to the polymer chain. Some $HO^\bullet$ deactivation occurs in an operating fuel cell through the reaction with H_2O_2 to generate H_2O and the more benign $HOO^\bullet$ radical, as shown in reaction 3 above. Fragmentation of the PFSA ionomers originates from the fraction of $HO^\bullet$ that escapes deactivation by H_2O_2. In order for the $HO^\bullet$ quenching system to be effective, several kinetic requirements must be fulfilled.

First, the deactivation chemistry must be faster than the reaction of $HO^\bullet$ with the PFSA membrane. For example, the rate constant of hydrogen atom abstraction from a perfluorocarboxylic acid intermediate (see SI) is estimated to be not greater than 1×10^6 M^{-1} s^{-1}. This reaction rate constant is quite slow and is expected to be a slow step in the degradation process. Of the reactions of $HO^\bullet$ given in Table 1, the reaction with Ce(III) is by far the fastest:[29,30] The corresponding reaction rate constant (the last entry in Table 1) has been determined in the presence of 0.4 M H_2SO_4 and $[H^+]$ is in excess.

Table 1. Reaction Rate Constants for the Hydroxyl Radical at 298 K

reaction	rate constant/(M^{-1} s^{-1})
$HO^\bullet + H_2O_2 \rightarrow HOO^\bullet + H_2O$	2.7×10^7 (ref 29)
$HO^\bullet + H_2 \rightarrow H^\bullet + H_2O$	4.3×10^7 (ref 29)
$HO^\bullet + R_fCF_2CO_2H \rightarrow H_2O + CO_2 + R_fC^\bullet F_2$	$< 1.0 \times 10^6$ (ref 30)
$HO^\bullet + Ce(III) + H^+ \rightarrow H_2O + Ce(IV)$	3×10^8 (ref 29)

Scheme 2. Fuel Cell Chemistry of Ce(IV) Reduction

$Ce(IV) + H_2O_2 \underset{k_{-1}}{\overset{k_1}{\rightleftharpoons}} Ce(III) + HOO^\bullet + H^+$	$k_1 = 1{\cdot}10^6$ $M^{-1}s^{-1}$
$Ce(IV) + HOO^\bullet \xrightarrow{k_2} Ce(III) + O_2 + H^+$	$k_2/k_{-1} = 13 \pm 2$
$2Ce(IV) + H_2 \xrightarrow{Pt} 2Ce(III) + 2H^+$	fast
$4Ce(IV) + 2H_2O \xrightarrow{Pt} 4Ce(III) + 4H^+ + O_2$	very slow

These considerations lead us to the first major conclusion: The absence of the DMPO/OH adduct in the MEA/Ce FC provides the evidence for the scavenging reaction of $HO^\bullet$ radicals by Ce(III). In addition, the absence of $HO^\bullet$ is expected to lead to the absence of the DMPO/CCR adducts.

The Presence of DMPO/OOH at the Cathode for CCV Operation. In an operating FC, the membrane is continuously bombarded by hydroxyl radicals; therefore an efficient deactivation scheme requires that the oxidized form of the quencher, (Ce(IV), be recycled to its reduced form for the repeated quenching chemistry. Furthermore, the recycling chemistry must also be faster that the degradation chemistry; this is the *second* kinetic requirement. As shown in Table 1, Ce(III) undergoes a facile redox reaction with $HO^\bullet$ radicals to produce H_2O and the corresponding oxidized cation Ce(IV).[29] Ce(IV) is a very strong oxidizing agent as indicated by its reduction potential of 1.72 V and, indeed, Ce(IV) is known to oxidize H_2O_2 to oxygen as shown in Scheme 2.[31−33] In addition to the uncatalyzed hydrogen peroxide-mediated reduction of Ce(IV) in a FC environment, Ce(IV) can also be catalytically reduced by both H_2 gas and H_2O. The last two pathways of Ce(IV) reduction require a Pt catalyst in the

membrane and although the H_2 reaction is facile, the oxygen evolution reaction is quite slow. The Pt catalyst of the cathode electrode is known to deposit within the membrane of an operating fuel cell over many hours of operation; however, we do not expect significant Pt deposition during our experiments because of the low relative humidity and relatively short operating times. Therefore, the reduction of Ce(IV) is expected to occur within the membrane via the reaction with H_2O_2, and not at the electrodes.

The available Ce(IV) reduction pathways are crucial to this highly effective mitigation system because it enables the hydroxyl radical quenching reactions to be accomplished with a small amount of Ce(III) additive.

The $HOO^{\bullet}$ radical is formed from the Ce(IV) oxidation of H_2O_2, as shown in Scheme 2. This rationale is consistent with earlier studies of Ce(IV) oxidation of H_2O_2 in a flow system at ambient temperature, where the $HOO^{\bullet}$ radicals were identified by direct ESR spectroscopy.[34] At this point, we cannot rule out that some of the trapped $HOO^{\bullet}$ radicals originate from the reaction of $HO^{\bullet}$ with H_2O_2 (reaction 2 above), although the relative rate constants and the high Ce(III) content argues against this explanation.

This part of the discussion leads to the next important conclusions: *The presence of the DMPO/OOH adduct in the MEA/Ce FC is evidence for and a result of the catalytic process involving the Ce(III)/Ce(IV) couple*, which is at the heart of membrane stabilization.[11] Moreover, the lower intensity of all adducts in the MEA/Ce FC is due to both the lower concentration of $HO^{\bullet}$ radicals, as well as to the lower reactivity of $HOO^{\bullet}$ radicals, as mentioned above. We note that the DMPO/OOH adduct was also detected in the MEA/H FC, but only after 240 min of CCV operation as seen in Figure 3 in ref 12, and not after "0 min" as in the MEA/Ce FC.

The Ce(III)/Ce(IV) couple redox chemistry is key for significant membrane stabilization with a low concentration of Ce(III). An understanding of the stabilization requirements may lead to additional neutralizing cations that prolong the lifetimes of fluorinated membranes in FCs; work along these lines is pursued in our laboratory.

DMPO/H and DMPO/D Adduct Formation. As seen in Figures 3 and 4, the DMPO/H and DMPO/D adducts were detected at the anode side even after short CCV operation times. The intensity of these signals is however much lower compared to that in the MEA/H FC. For MEA/H we have proposed that the DMPO/H and DMPO/D adducts could be formed by trapping H and D atoms formed by reaction of the H_2 and D_2 with $HO^{\bullet}$.[12] The lower concentration of the $H^{\bullet}$ and $D^{\bullet}$ adducts in the MEA/Ce FC may be due to a lower concentration of $HO^{\bullet}$ radicals.

An additional reason for the low intensities of the DMPO/H and DMPO/D adducts may be possible: Hydrogen atom is a very strong oxidizing agent (reduction potential = 2.30 V)[35,36] and is therefore capable of oxidizing Ce(III) during its reduction to hydrogen gas, as shown in reaction 4 below. Thus, if hydrogen atoms are formed in MEA/Ce, they could be scavenged by Ce(III) and not be available for trapping.

$$H^{\bullet} + Ce(III) + H^{+} \rightarrow H_2 + Ce(IV) \qquad (4)$$

The detection of both DMPO/H and DMPO/D adducts when operating the fuel cell with D_2 at the anode remains an unresolved issue.

Conclusions

We have presented experiments at 300 K in an in situ fuel cell inserted in the resonator of an ESR spectrometer. The in situ fuel cell was operated with a Nafion 117 membrane 10% neutralized by Ce(III) (notation MEA/Ce) and covered on both sides by Pt as catalyst (coverage 0.2 mg/cm^2), at closed and open circuit voltage (CCV and OCV) conditions. Experiments with hydrogen or deuterium at the anode, and oxygen at the cathode were performed.

The presence of the radicals was determined by addition of 5,5-dimethylpyrroline-*N*-oxide (DMPO) as a spin trap, and simulation of the spectra from the DMPO adducts. The main objective of these experiments was to visualize early events in the mitigation mechanism of Ce(III) on the membrane degradation. To this end, the present results were compared to those obtained in an in situ FC based on Nafion 117 in the acid form (notation MEA/H).[12]

The main differences between the two types of experiments are significant. (a) The dominant adducts are different: DMPO/OH for the MEA/H FC ($a_N = a_H = 14.8$ G) and DMPO/OOH for MEA/Ce FC ($a_N = 13.7$ G and $a_H = 11.7$ G). (b) The DMPO/CCR adduct, the adduct of a carbon-centered radical derived from the membrane, is absent for the MEA/Ce FC, and present in the absence of Ce(III). (c) The intensity of all adducts is much lower in the MEA/Ce FC.

The absence of the $HO^{\bullet}$ radicals was explained by their scavenging with Ce(III): $HO^{\bullet} + Ce(III) + H^{+} \rightarrow H_2O + Ce(IV)$. A lower $HO^{\bullet}$ concentration is expected to explain the absence of DMPO/CCR in the MEA/Ce FC. The presence of the DMPO/OOH adduct was rationalized by the oxidation of H_2O_2 with Ce(IV): $Ce(IV) + H_2O_2 \leftarrow Ce(III) + HOO^{\bullet} + H^{+}$. The lower intensity of all adducts is a result of the replacement of $HO^{\bullet}$ by the less aggressive $HOO^{\bullet}$ radical in the MEA/Ce compared to $HO^{\bullet}$ in MEA/H.

The DMPO/H and DMPO/D adducts were detected for CCV operation at both the cathode and the anode. It was previously suggested[12] that $H^{\bullet}$ and $D^{\bullet}$ may abstract the fluorine attached to the tertiary carbon of the membrane; the absence of the carbon-centered adduct in the MEA/Ce-based FC suggests that this process is not effective at 300 K. The reaction with O_2 to form $HOO^{\bullet}$ may also impose limits on the lifetimes of the $H^{\bullet}$ and $D^{\bullet}$ atoms in a FC.

Acknowledgment. This study was supported by the Polymers Program of the National Science Foundation and the General Motors Electrochemical Energy Research Lab. We thank Dr. Cortney Mittelsteadt of Giner Electrochemical Systems LLC for the gift of the MEA/Ce based on the Nafion® 117 membranes.

Supporting Information Available: Scheme S1, presenting the generalized PFSA main chain unzipping mechanism, Figure S1 giving a schematic drawing of the in situ fuel cell, and Figure S2, presenting experimental and simulated ESR spectra of DMPO adducts when the spin trap was added after 240 min of CCV operation in the MEA/H FC. This material is available free of charge via the Internet at http://pubs.acs.org.

References and Notes

(1) *Fuel Cells—Green Power*, Los Alamos National Laboratory. See also website: www.education.lanl.gov/resources/fuelcells.
(2) Kinumoto, T.; Inaba, M.; Nakayama, Y.; Ogata, K.; Umebayashi, R.; Tasaka, A.; Iriyama, Y.; Abe, T.; Ogumi, Z. *J. Power Sources* **2006**, *158*, 1222–1228.
(3) (a) Walling, C. *Acc. Chem. Res.* **1975**, *8*, 125–131. (b) Sawyer, D. T.; Sobkowiak, A.; Matsushita, T. *Acc. Chem. Res.* **1996**, *29*, 409–416. (c) Walling, C. *Acc. Chem. Res.* **1998**, *31*, 155–157. (d) Goldstein, S.; Meyerstein, D. *Acc. Chem. Res.* **1999**, *32*, 547–550.
(4) Adzic, R. In *Electrocatalysis*; Lipkowski, J., Ross, P. N., Eds.; Wiley-VCH: New York, 1998; Chapter 5, pp 197−242.
(5) Kadirov, M. K.; Bosnjakovic, A.; Schlick, S. *J. Phys. Chem. B* **2005**, *109*, 7664–7670.
(6) Lund, A.; Macomber, L.; Danilczuk, M.; Stevens, J.; Schlick, S. *J. Phys. Chem. B* **2007**, *111*, 9484–9491.

(7) Danilczuk, M.; Coms, F. D.; Schlick, S. *Fuel Cells* **2008**, *8*, 436–452.
(8) Ghassemzadeh, L.; Marrony, M.; Barrera, R.; Kreuer, K. D.; Maier, J.; Müller, K. *J. Power Sources* **2009**, *186*, 334–338.
(9) Endoh, E. *ECS Trans.* **2008**, *16*, 1229–1240.
(10) Trogadas, P.; Parrondo, J.; Ramani, V. *Electrochem. Solid State Lett.* **2008**, *11*, B113–B116.
(11) Coms, F. D.; Liu, H.; Owejan, J. E. *ECS Trans.* **2008**, *16*, 1735–1747.
(12) Danilczuk, M.; Coms, F. D.; Schlick, S. *J. Phys. Chem. B* **2009**, *113*, 8031–8042.
(13) Janzen, E. G. *Acc. Chem. Res.* **1971**, *4*, 31–40.
(14) Lagercrantz, C. *J. Phys. Chem.* **1971**, *75*, 3466–3475.
(15) Bosnjakovic, A.; Kadirov, M. K.; Schlick, S. *Res. Chem. Intermed.* **2007**, *33*, 677–687.
(16) Bosnjakovic, A.; Schlick, S. *J. Phys. Chem. B* **2006**, *110*, 10720–10728.
(17) The software WinSim can be accessed at: http://www.niehs.nih.gov/research/resources/software/tools/index.cfm.
(18) Abragam, A.; Bleaney, B. *Electron Paramagnetic Resonance of Transition Ions*: Clarendon Press: Oxford, U.K., 1970; pp 307−312.
(19) Panchenko, A.; Dilger, H.; Kerres, J.; Hein, M.; Ullrich, A.; Kaz, T.; Roduner, E. *Phys. Chem. Chem. Phys.* **2004**, *6*, 2891–2894.
(20) Panchenko, A.; Dilger, H.; Moller, E.; Sixt, T.; Roduner, E. *J. Power Sources* **2004**, *127*, 325–330.
(21) Madden, K. P.; Taniguchi, H. *J. Phys. Chem.* **1996**, *100*, 7511–7516.
(22) Curtin, D. E.; Lousenberg, R. D.; Henry, T. J.; Tangeman, P. C.; Tisack, M. E. *J. Power Sources* **2004**, *131*, 41–48.
(23) Healy, J.; Hayden, C.; Xie, T.; Olson, K.; Waldo, R.; Brundage, A.; Gasteiger, H.; Abbott, J. *Fuel Cells* **2005**, *5*, 302–308.
(24) Borup, R.; Meyers, J.; Pivovar, B.; Kim, Y. S.; Mukundan, R.; Garland, N.; Myers, D.; Wilson, M.; Garzon, F.; Wood, D.; Zelenay, P.; More, K.; Stroh, K.; Zawodinski, T.; Boncella, J.; McGrath, J. E.; Inaba, M.; Miyatake, K.; Hori, M.; Ota, K.; Ogumi, Z.; Miyata, S.; Nishikate, A.; Siroma, Z.; Uchimoto, Y.; Yasuda, K.; Kimijima, K. I.; Iwashita, N. *Chem. Rev.* **2007**, *107*, 3904–3951.
(25) Zhou, C.; Guerra, M. A.; Qiu, Z.-M.; Zawodinski, T. A.; Schiraldi, D. A. *Macromolecules* **2007**, *40*, 8695–8707.
(26) Ramaswarmy, N.; Hakim, N.; Mukerjee, S. *Electrochem. Acta* **2008**, *53*, 3279–3295.
(27) Coms, F. D. *ECS Trans.* **2008**, *16*, 235–255.
(28) Spulber, M.; Schlick, S. Unpublished results.
(29) Buxton, G. V.; Greenstock, C. L.; Helman, W. P.; Ross, A. B. *J. Phys. Chem. Ref. Data* **1988**, *17*, 513–886.
(30) Maruthamuthu, P.; Padmaja, S.; Huie, R. E. *Int. J. Chem. Kinet.* **1995**, *27*, 605–612.
(31) Davies, G.; Kirschenbaum, L. J.; Kustin, K. *Inorg. Chem.* **1968**, *7*, 146–154.
(32) Czapski, G.; Bielski, B. H.; Sutin, N. *J. Phys. Chem.* **1963**, *67*, 201–203.
(33) Mahlman, H. A.; Matthews, R. W.; Sworski, T. J. *J. Phys. Chem.* **1971**, *75*, 250–255.
(34) Saito, E.; Bielski, B. H. J. *J. Am. Chem. Soc.* **1961**, *83*, 4467–4468.
(35) Schwarz, H. A. *J. Chem. Educ.* **1981**, *58*, 101–105.
(36) The one electron reduction reaction of the hydrogen atom leads to the formation of H^- in the absence of protons. The corresponding potential, $E_0 = 2.30$ V, is defined at an H^+ activity of 1, or 1.0 M, pH = 0. Under these conditions (which are relevant to fuel cells), the product of the one electron hydrogen reduction is molecular hydrogen: $H^\bullet + e^- + H^+(1\ M) \rightarrow H_2(g)$. The reduction potential is pH dependent, and at higher pH the reduction potential will be lower.